Available online at www.sciencedirect.com
SCIENCE DIRECT®
Journal of Photochemistry and Photobiology A: Chemistry 163 (2004) 277–280
Journal of Photochemistry and Photobiology A:Chemistry
www.elsevier.com/locate/jphotochem

Effect of calcination atmosphere on TiO_2 photocatalysis in hydrogen production from methanol/water solution

Nae-Lih Wu*, Min-Shuei Lee, Zern-Jin Pon, Jin-Zern Hsu

Department of Chemical Engineering, National Taiwan University, Taipei 106, Taiwan

Received 23 September 2003; received in revised form 1 December 2003; accepted 12 December 2003

Abstract

TiO_2 photocatalysts were synthesized by a sol–gel process followed by calcination at 400 °C in Ar, air, N_2, H_2 (3% in N_2) and vacuum ($\sim 5 \times 10^{-3}$ torr), respectively. Toward H_2 production from a water/methanol (vol. ratio = 1.4/1) solution, the catalysts exhibited activities in the order, according to calcination atmosphere, of Ar > air > N_2 > vacuum ~ H_2. The low activity resulting from either vacuum or H_2 calcination was ascribed to a reduced coverage of surface hydroxyl and high bulk defect density, based on the X-ray photoelectron and UV-Vis spectroscopic analyses, while the high activity from Ar calcination is to enhanced visible-light excitation.

Keywords: TiO_2; Phototcatalysis; Hydrogen production; Methanol; Calcination atmosphere; X-ray photoelectron spectroscopy

1. Introduction

Because of its high chemical stability and favorable energy band structure, TiO_2 has drawn tremendous attention for its potential applications in photocatalysis in different fields. The photocatalytic performance of TiO_2 is well known to depend not only on its bulk energy band structure but, to a great extent, on the surface property. The type and density of surface state are affected by, among others, the synthesis process. A soft mechanical treatment of TiO_2 powder, for instance, was found to significantly reduce its photocatalytic activity for Cr(VI) reduction [1], while treatment in either H_2- or N_2-plasma to enhance the activity within the visible-light range for certain reactions [2,3]. The interplay between processing condition and photocatalytic activity remains largely a state-of-art and beyond prediction at this point. Crystalline TiO_2 has typically been calcined and/or crystallized in oxidizing atmospheres, such as air and oxygen. The effect of the so-called "inert" atmospheres, such as N_2, Ar, and vacuum, has mostly been overlooked.

In the present work, we studied the effect of calcination atmospheres, including Ar, air, N_2, H_2 and vacuum ($\sim 5 \times 10^{-3}$ Torr), on the photocatalytic properties of TiO_2, using photocatalytic H_2 production from methanol/water solution as the chemical probe. For H_2 production from water, many studies have concluded that direct photodecomposition of water into H_2 and O_2 has a very low efficiency due to rapid reverse reaction. A much higher hydrogen production rate can be obtained by addition of a "sacrificial reagent," which is oxidized to a product that is less reactive toward hydrogen. In the case of TiO_2-catalyzed photodecomposition of methanol (MeOH) and water solution, it was suggested [4] that the holes generated by light would oxidize MeOH to HCHO, HCO_2H and eventually to CO_2, according to the following serial reaction schemes:

$$\mathrm{MeOH_{(l)} \overset{h\nu,\mathrm{catal}}{\leftrightarrow} HCHO_{(g)} + H_{2(g)}}, \quad \Delta G_1^\circ = 64.1\,\mathrm{KJ/mole} \tag{1}$$

$$\mathrm{HCHO(g) + H_2O(l) \overset{h\nu,\mathrm{catal}}{\leftrightarrow} HCO_2H_{(l)} + H_{2(g)}}, \quad \Delta G_2^\circ = 47.8\,\mathrm{KJ/mole} \tag{2}$$

$$\mathrm{HCO_2H_{(l)} \overset{h\nu,\mathrm{catal}}{\leftrightarrow} CO_{2(g)} + H_{2(g)}}, \quad \Delta G_3^\circ = -95.8\,\mathrm{KJ/mole} \tag{3}$$

The first two reactions, both having a positive Gibbs energy [5], are thermodynamically unfavorable at room temperature, and photon irradiation is to provide work to raise the chemical potential of the reactant sides in order to drive the reactions to the right. Under the same irradiating condition in practice, the amount of effective energy the reacting system will receive varies with the efficiency of the photocatalyst to pass the photon energy to the reaction system. It is

* Corresponding author. Tel.: +886-2-23627158; fax: +886-2-23623040.
E-mail address: nlw001@ntu.edu.tw (N.-L. Wu).

1010-6030/$ – see front matter © 2004 Elsevier B.V. All rights reserved.
doi:10.1016/j.jphotochem.2003.12.009

the third reaction, which has a large negative Gibbs energy, intrinsically provides a barrier for reverse consumption of generated hydrogen.

In brief, the photocatalytic activity of TiO_2 was found to depend heavily on the calcination atmosphere, showing more than ten-fold variation, with the lowest and highest activities resulting from H_2- and Ar-calcination, respectively. The relations between the reactivity and the surface and bulk electronic properties, as revealed by X-ray photoelectron spectroscopic (XPS) and ultraviolet-visible (UV-Vis) spectroscopic analyses, were discussed.

2. Experimental

TiO_2 powder was synthesized by a conventional sol–gel process. $TiCl_4$ was first dissolved in an ethanol/water (volume ratio = 4 : 1) solution, and ammonia was then introduced into the solution to induce condensation until pH reached 7.5. The resulted gelatinous precipitate was filtered and washed to reduce $[Cl^-]$ to below 5×10^{-4} M, as determined by ion chromatography, and then dried at 65 °C in air. Calcination of xerogel was carried out in Ar, synthetic air (N_2/O_2 mol ratio = 79 : 21), nitrogen, hydrogen (3 mol.% in N_2), and vacuum ($\sim 5 \times 10^{-3}$ Torr), respectively. The gases used have a purity of 99.9% or better. Half gram of the oxide powder was loaded on an Al_2O_3 boat and placed at the center of a tubular furnace, which has a dimension of 80 cm L × 5 cm D. Calcination procedure started with purging the reactor with the selected gas at 0.5 L/min (in the case of vacuum treatment, the reactor was evacuated to $\sim 5 \times 10^{-3}$ Torr) for 1 h, heated the powder at a rate of 100 °C/h to 400 °C, and held the powder at 400 °C for 1 hr before finally the powder being furnace-cooled. For the commercial crystalline TiO_2 catalyst (P25, Degussa), it was used as received.

Kinetic studies were carried out by using a vertical tubular batch reactor made of quartz. During the experiment, the entire reactor was enclosed inside a UV-light house (Rayonet photochemical reactor, RPR-100), and the reactor was half-filled with a water/MeOH (H_2O/MeOH vol. ratio = 1.4 : 1) solution, in which the oxide particles, in an amount of 1.25 g/l, were constantly dispersed by a magnetic stirrer. The light house was equipped with 16 UV-light (with the maximum intensity at 300 nm wavelength) tubes, each having a power of 12 W. The unfilled space above the solution was evacuated at the beginning of reaction, and the H_2 concentration was determined intermittently by extracting a small volume of the gas-phase product for gas chromatography (GC) analysis. The accumulative H_2 production data were then calculated from the concentration data, assuming ideal-gas behavior.

X-ray diffraction (XRD; Mac-Science/ MXP3) was employed to determine the crystalline phase and grain size of the TiO_2 powders. X-ray photoelectron spectroscopic (XPS) analysis was carried out on a spectrometer (MT 500, VG Microtech) equipped with a Mg Kα X-ray source. Diffuse reflectance ultraviolet-visible (UV-Vis) spectroscopic analysis was conducted on a Hitachi U3410 spectrometer, which is equipped with an integration sphere and PbS and photomultiplier detectors for photon detection. Deuterium and tungsten iodide lamps are used as the light sources for wavelength ranges of 185–340 and 340–2500 nm, respectively. The spectra were acquired at room temperature with $BaSO_4$ as the reference.

3. Results and discussion

The synthesized catalysts contain only anatase phase and have crystallite sizes in the range of 9.0–10.0 nm (Table 1) and similar BET surface areas of ~110 (±5%) m^2/g. For kinetic study, a small amount of H_2 was detected from the solution even without the catalyst. Nevertheless, H_2 production was greatly enhanced with the presence of the TiO_2 catalysts. As shown in Fig. 1, upon UV-irradiation, H_2 was produced with steadily increasing concentration with time until it saturated at a steady level. In a batch reactor, such as

Table 1
Crystallite size and kinetic data of TiO_2 catalyst

Calcination atmosphere	Crystallite size[a] (nm)	P_{eq} (μmole)[b]	$dP/dt\|_{max}$ (μmole/min)[b]	t_{max} (min)[b]
Ar	9.8	1515.4	30.2	0
Air	9.0	1109.2	7.1	53.0
N_2	10.0	1182.9	5.0	57.8
Vacuum	9.1	1053.4	2.9	199.0
H_2	9.8	579.4	3.2	121.1

[a] Crystallite size were calculated from (1 0 1) XRD reflection of anatase based on Debye–Scherrer equation.

[b] P_{eq}, $dP/dt|_{max}$, and t_{max} are, respectively, the equilibrium (i.e. saturation) accumulative production, maximum hydrogen generation rate, and maximum-rate reaction time, respectively, determined based on the fitting by Boltzman equation.

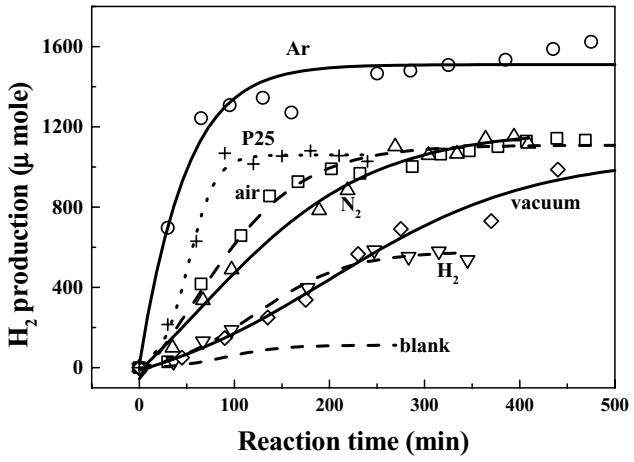

Fig. 1. H_2 generation curves. The data sets are indexed according to calcination atmosphere except for that of the commercial catalyst, indexed as P25. The dashed line is for the experiment without any catalyst. The lines are fitted using Boltzman equation.

the one currently employed, a steady state represents equilibrium.

It was found that all these curves can be satisfactorily fitted by the Boltzman equation, having a form of

$$P = P_{eq} + \frac{(A - P_{eq})}{\{1 + \exp[(t - t_0)/\delta]\}}$$

where P is the accumulative hydrogen production (in μmole) within the open space in the reactor, P_{eq}, the equilibrium (i.e. saturation) accumulative production, t, the reaction time (min), and A, t_0, and δ are parameters. Mathematically, this equation gives a curve containing a deflection point at t_0. For $t_0 > 0$, the maximum hydrogen generation rate, $dP/dt|_{max}$, occurs at the deflection point, and hence the maximum-rate reaction time, t_{max}, is equal to t_0. For $t_0 \leq 0$, however, it means in reality that the maximum rate occurs at the very beginning of the reaction, i.e. $t_{max} = 0$. The fitted $dP/dt|_{max}$, t_{max}, and P_{eq} data are summarized in Table 1.

The H_2-calcined catalyst was found to exhibit the worst performance; it exhibited the lowest reaction rate as well as the lowest equilibrium production (Fig. 1; Table 1). The vacuum-calcined catalyst exhibited about the same reaction rate within the initial reaction period but enabled a much higher equilibrium production level after long reaction time. One reasonable explanation to the difference in their P_{eq} is that these two catalysts have similar photocatalytic activity toward the forward reactions but with the vacuum-calcined catalyst being less active toward the reverse reactions.

The air- and N_2-calcined catalysts showed another level of performance. They both exhibited maximum rates that are nearly twice those of the H_2 and vacuum samples (Table 1) with the air-sample being even slightly superior to the N_2 one. The Ar-calcined catalyst, on the other hand, gave overall the best performance in terms of both the maximum rate and equilibrium production level. It is also superior to the commercial P25 catalyst.

Fig. 2 shows the diffuse reflectance UV-Vis spectra. The absorption edge energy is determined by Tauc plot [$(\alpha h\nu)^2$ versus $h\nu$, where α is the absorbance] for semiconductors with the direction transition (Fig. 2, the inset) [6–9]. Except for the vacuum-calcined catalyst, which appears black, all the catalysts show a sharp UV absorption near 3.25 eV, consistent with the theoretical band gap energy of anatase TiO_2. Significant differences, however, exist in absorption within the visible-light range next to the absorption edge. The Ar, air and N_2 samples showed visible-light absorption correlated consistently with their activities, showing increasing activity with increasing absorption. On the other hand, the vacuum and H_2 samples both showed stronger visible-light absorptions but yet lower activities than the rest catalysts. Powder darkening upon heat treatment in vacuum is not unique to TiO_2 but has previously been known for other wide-band gap oxides including SnO_2 and ZrO_2 as well [10–12]. While it is generally agreed that this phenomenon is associated with oxygen deficiency, the nature of the coloring center(s) remains controversial [10,12]. It was further

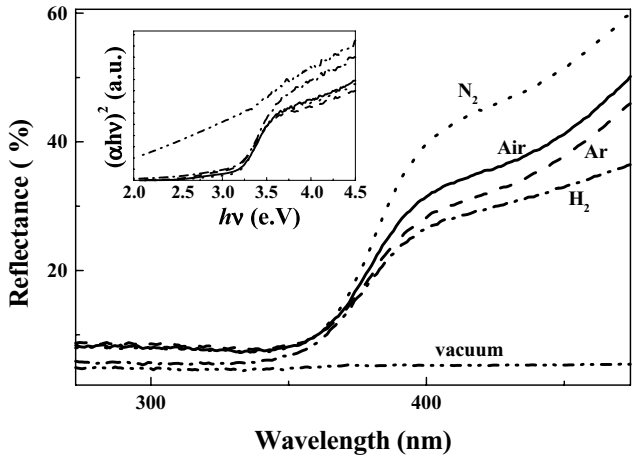

Fig. 2. Diffuse reflectance spectra of TiO_2 catalysts. The lines are indexed according to calcination atmosphere. The inset shows the $(\alpha h\nu)^2$ vs. $h\nu$ plots, where α is absorbance.

noticed that the vacuum-calcined powder turned white upon subsequent anneal in air, i.e. the darkening process is reversible.

XPS studies indicated mainly two types of surface properties. The Ar- and air-calcined catalysts showed higher Ti and O binding energies than the other catalysts (Fig. 3). The binding energies of Ti (459.7 ± 0.2 eV for Ti $2P_{3/2}$) for the Ar and air samples are typical of Ti^{4+} [13,14]. A red shift by ~2.2 eV observed on the other samples indicates the presence of Ti ions of lower valences therein. This is consistent with the electron spin resonance analysis by Serwicka [15], who detected the presence of Ti^{3+} on vacuum-reduced TiO_2 at 400–500 °C. For the O (1s) XPS peak, it is typical of the convolution of peaks from lattice O and surface hydroxyl. Wang et al. [13], in studying the UV light-induced hydrophilic properties of TiO_2, observed a blue shift of O

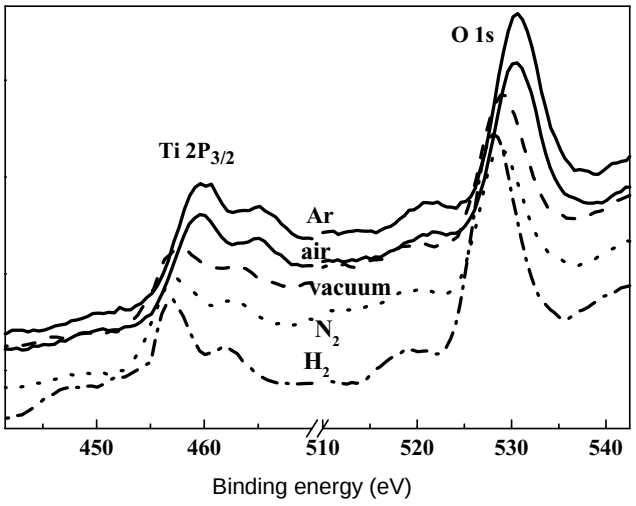

Fig. 3. XPS spectra of TiO_2 catalysts. Shown are Ti ($2P_{3/2}$) and O (1s) peaks. The lines are indexed according to calcination atmosphere.

(1s) peak by 1.5–2.6 eV as the amount of surface hydroxyl group increases. The O (1s) binding energy difference observed in the present study is 1.7 eV, and it is believed to be due to the same cause. That is, the air- and Ar calcined catalysts have a higher surface coverage of hydroxyl group than the other catalysts.

Wang et al. [13] also noted that, while the OH coverage was increased by UV-irradiation, the valence of Ti ions remained essentially unchanged. Similar effect was also observed by ion beam irradiation [14]. An OH-enrichment mechanism involving oxygen vacancies created by hole-trapping was proposed by Sakai et al. [16]. Our XPS results, on the other hand, indicate that the oxygen non-stoichiometry due to thermal treatment in a non-oxidizing atmospheres, including N_2, vacuum and H_2, results in Ti ions of lower valences, most likely Ti^{3+} (Fig. 3), but does not contribute to the formation of surface hydroxyl.

For a semiconductor-photocatalyzed reaction, the reaction rate is basically determined by how fast the charged particles, including the valence-band hole and conduction-band electron, are generated and the how efficiently they are transferred to the reactants at surface before they recombine. Our UV-Vis spectroscopic data (Fig. 2) have shown that all the currently synthesized catalysts exhibited significant absorption of visible-light. The occurrence of this absorption is known to be caused by the presence of structural defects that possess energy state within the band gap. Two opposite effects related to photocatalysis could result from them. On the one hand, these defects could enable excitation with photon energy lower than the band gap energy and hence facilitates excitation to form the charged particles. On the other, they would also act as scattering centers to slow down the transport of charged particles to surface where reaction takes place. As a result, an optimum density, as well as an optimum property, of the structure defect is expected for good photocatalysis performance. This may explain the observation that there appears to be an optimum visible-light absorption level for maximum reaction rate (Fig. 2). For the Ar, air and N_2 samples, the photocatalytic activity was found to increase with increasing the absorption. This may suggest that the defect density is low enough that the excitation effect is predominant. In contrast, the excitation effect might be severely offset by the scattering effect in the cases of the vacuum and H_2 samples, which showed very strong visible-light absorptions but yet poor performance.

Another strong clue to the cause of the reactivity variation is provided by the XPS data, which showed difference in the surface hydroxyl coverage. It has been pointed out [17,18] that >TiOH, the so-called surface “titanol” group, is an important trapping center for the valence-band hole and hence the principal oxidizing site in the photoactivated TiO_2. Reduced hydroxyl coverage would thus impair the activity of the catalyst. This might also contribute, in part, to the poor performance exhibited by the vacuum- and H_2-calcined samples. An intermediate level of visible-light absorption level combined with high surface hydroxyl coverage render the Ar-calcined catalyst the highest photocatalytic activity.

In summary, calcination atmosphere has been found to have significant effects on the photocatalytic acitivity of TiO_2 in hydrogen production from methanol/water solution. Calcination in either hydrogen or vacuum results in a high defect density and low surface hydroxyl coverage, giving low activity. Calcination in Ar, in contrast, enhances visible-light excitation and high hydroxyl coverage, leading to high activity.

Acknowledgements

The work is supported by the National Science Council and Department of Industrial Technology of Republic of China under contract numbers 91-2214-E-002-007 and 92-EC-17-A-09-S1-019, respectively.

References

[1] M.C. Hidalgo, G. Colon, J.A. Navio, J. Photochem. Photobiol. A: Chem. 148 (2002) 341–348.
[2] I. Nakamura, N. Negishi, S. Kutsuna, T. Ihara, S. Sugihara, K. Takeuchi, J. Mol. Catal. A: Chem. 161 (2000) 205–212.
[3] R. Asahi, T. Morikawa, T. Ohwaki, K. Aoki, Y. Taga, Science 293 (2001) 269–271.
[4] T. Kawai, T. Sakata, J.C.S. Chem. Commun. (1980) 694–695.
[5] D.R. Lide (Ed.), Handbook of Chemistry and Physics, 83rd ed., CRC Press, Boca Raton, FL, 2002, pp. 5-1–5-60.
[6] J. Tauc, in: J. Tauc (Ed.), Amorphous and Liquid Semiconductors, Plenum Press, NY, 1974, pp. 159–220.
[7] Y. Wang, A. Suna, M. Mahler, R. Kasowski, J. Chem. Phys. 87 (1987) 7315–7322.
[8] N. Nicoloso, A. Lobert, B. Leibold, Sens. Actuators B 8 (1992) 253–256.
[9] I. Kosacki, V. Petrovsky, H.U. Anderson, Appl. Phys. Lett. 74 (1999) 341–343.
[10] G.M. Ingo, J. Am. Ceram. Soc. 74 (1991) 381–386.
[11] N.L. Wu, L.F. Wu, I.A. Rusakova, A. Hamed, A.P. Litvinchuk, J. Am. Ceram. Soc. 82 (1999) 67–73.
[12] X.G.Y.Q. Sun, K. Cui, Sens. Actuators B 31 (1996) 139–145.
[13] R. Wang, N. Sakai, A. Fujishima, T. Watanabe, K. Hashimoto, J. Phys. Chem. B 103 (1999) 2188–2194.
[14] M. Takeuchi, Y. Onozaki, Y. Matsumura, H. Uchida, T. Kuji, Nuclear Instrum. Meth. Phys. Res. B 206 (2003) 259–263.
[15] E. Serwicka, Colloids Surf. 13 (1985) 287.
[16] N. Sakai, A. Fujishima, T. Watanabe, K. Hashimoto, J. Phys. Chem. B 105 (2001) 3023–3026.
[17] M.R. Hoffmann, S.T. Martin, W.Y. Choi, D.W. Bahnemann, Chem. Rev. 95 (1995) 69–96.
[18] Z. Zhang, C.C. Wang, R. Zakaria, J.Y. Ying, J. Phys. Chem. B 102 (1998) 10871–10878.